Author's Accepted Manuscript

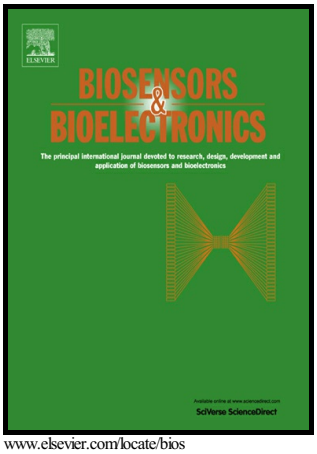

www.elsevier.com/locate/bios

A Novel Electrogenerated chemiluminescence Biosensor for Histone Acetyltransferases Activity Analysis and Inhibition Based on Mimetic Superoxide Dismutase of Tannic Acid assembled nanoprobes

Yan Zou, Zonghua Wang, Huixin Zhang, Yang Liu

PII: S0956-5663(18)30741-3
DOI: https://doi.org/10.1016/j.bios.2018.09.048
Reference: BIOS10788

To appear in: *Biosensors and Bioelectronic*

Received date: 13 August 2018
Accepted date: 12 September 2018

Cite this article as: Yan Zou, Zonghua Wang, Huixin Zhang and Yang Liu, A Novel Electrogenerated chemiluminescence Biosensor for Histone Acetyltransferases Activity Analysis and Inhibition Based on Mimetic Superoxide Dismutase of Tannic Acid assembled nanoprobes, *Biosensors and Bioelectronic,* https://doi.org/10.1016/j.bios.2018.09.048

This is a PDF file of an unedited manuscript that has been accepted for publication. As a service to our customers we are providing this early version of the manuscript. The manuscript will undergo copyediting, typesetting, and review of the resulting galley proof before it is published in its final citable form. Please note that during the production process errors may be discovered which could affect the content, and all legal disclaimers that apply to the journal pertain.

ACCEPTED MANUSCRIPT

A Novel Electrogenerated chemiluminescence Biosensor for Histone Acetyltransferases Activity Analysis and Inhibition Based on Mimetic Superoxide Dismutase of Tannic Acid assembled nanoprobes

Yan Zou[a,b], *Zonghua Wang*[b*], *Huixin Zhang*[a], *Yang Liu*[a*]

[a]Department of Chemistry, Beijing Key Laboratory for Analytical Methods and Instrumentation, Kay Lab of Bioorganic Phosphorus Chemistry and Chemical Biology of Ministry of Education, Tsinghua University, Beijing 100084, China.

[b]Shandong Sino-Japanese Center for Collaborative Research of Carbon Nanomaterials, College of Chemistry and Chemical Engineering, Qingdao University, Qingdao, Shandong, 266071, China.

wangzonghua@qdu.edu.cn

liu-yang@mail.tsinghua.edu.cn

[*]Corresponding authors. Tel.: 86-10-62798187; fax: 86-10-62771149

Accepted manuscript

ACCEPTED MANUSCRIPT

Abstract

A simple and sensitive turn-off electrogenerated chemiluminescence (ECL) biosensor was designed for the analysis of histone acetyltransferases (HATs) activity and inhibitor evaluation based on the anti-hydrolysis ability of acetylated peptide and mimetic superoxide dismutase (SOD) features of tannic acid (TA) assembled gold nanoparticles (AuNPs) nanoprobes. In this strategy, after the acetylated reaction in the presence of HATs, the acetylated peptide on electrode was resistance to the hydrolysis of trypsin, and can absorb AuNPs@TA-Fe probe onto the electrode by the hydrophobic interaction and hydrogen bonding interaction. Thus, the ECL signal of the modified electrode in luminol solution decreased significantly owing to the mimetic SOD features of the TA assembled nanoprobe that can eliminate the reactive oxygen species. The ECL intensity changes can be utilized for sensitive HATs activities detection and inhibitor screening. The detection limit of the as-prepared ECL biosensor was 0.074 nM (S/N = 3). Moreover, the as designed ECL biosensor was also applied in MCF-7 cell lysates for HATs activity analysis and drug inhibition, which is feasible to HATs activity analysis and inhibitor screening, and presents highly promise in HAT-related clinical diagnostics.

Keywords: Acetyltransferase, Mimetic enzyme, Tannic acid, Electrogenerated chemiluminescence biosensor

Accepted manuscript

ACCEPTED MANUSCRIPT

1. Introduction

In the eukaryotic chromatins, histone proteins and DNA can constitute its basic block. The histone proteins can be acetylated in the presence of histone acetyltransferases (HATs), which is an important post-translational modification (PTM). It not only is an essential regulatory mechanism in epigenetic system but also controls the transcriptional and structural state of chromatin. (Li et al. 2016; Zhen et al. 2012; Kim et al. 2000) Furthermore, in many basic biological processes, such as genome stability, histone deposition, DNA replication and repair, and nutrient metabolism, the acetylation reaction also plays a vital role. (Dancy et al. 2015; Ghadiali et al. 2011) Lysine residues on histone proteins, which is important acetylation site, can be acetylated by HATs and the charge of histone proteins was changed from positive to neutral. The phenomenon influences the chromatin structure and gene expression. Up to now, many studies have showed many clinical diseases, such as cancers, HIV infection, neurological disorders, and inflammatory, etc, their pathogenesis has tight association with aberrant HATs activities. (Han et al. 2015; Han et al. 2015) What's more, these clinical diseases have regarded HATs as significant biomarkers, and HATs inhibitors also show contribution to the chemotherapy as well as discovery of anti-cancer drugs. As a result, reliable, feasible and sensitive approaches for detecting HATs activity and its inhibitors screening are of paramount importance for HATs-related biochemical research and clinical diagnostics.

For detecting HATs activity, researchers mainly relies on radioisotope labelling of histone substrates decades ago, which is limited by the tedious procedures, radioactive substances wastes and hazards. (Xie et al. 2009) In recent years, some techniques including electrochemical approach, chemiluminescence and fluorescence analyses were also applied in the field of HATs activities analysis. (Zhen et al. 2012; Han et al. 2015; Han et al. 2015; Xie et al. 2009) By the antibody recognition of acetylated lysine sites or the variation in charge, anti-hydrolytic ability and nucleophilicity, the HATs activity was detecting using above analysis approaches. (Kim et al. 2000) In addition, in order to reflect the activity of HATs, a few methods are also proposed for

Accepted manuscript

ACCEPTED MANUSCRIPT

quantifying the by-products (coenzyme A (Co A)). (Hu et al. 2015; Chen et al. 2015) Although the existing detection approaches afford obvious specificity, efficiency and stability for probing HATs activity, considering long time spending of tedious procedures, high spending of antibodies, danger of labelling technique, and photo-bleaching of fluorescence, etc, a novel, safe, rapid and sensitive method for detecting HATs activity is also highly needed.

In recent years, due to its advantages including rapidness, easy controllability, highly sensitive and low cost, electrogenerated chemiluminescence (ECL) has attracted a lot of attention and been used in various field, such as immunoassay, environmental detection, enzyme reaction and clinical diagnosis. (Li et al. 2004; Zhang et al. 2007; Zhang et al. 2004; Yang et al. 2016; Qi et al. 2014; Divsar et al. 2011; Shi et al. 2010; Chen et al. 2013; Li et al. 1996; Lu et al. 2006; Hu et al. 2007) The ECL phenomenon was arises from the electron-transfer reaction between electrogenerated species at electrode surfaces and the ECL technique is also processing and developing. Due to their superior photo-electrochemical properties, plenty of nanmomaterials based nanoprobes were prepared for ECL biosensor fabrication (Wang et al. 2013; Wang et al. 2014; Zhang et al. 2010; Forzani et al. 2009; He et al. 2015; Wang et al. 2013; Yang et al. 2015; Liu et al. 2012; Chen et al. 2014). For example, a simple sandwich ECL biosensor was build using concanavalin A (Con A)-integrating gold-nanoparticle-modified $Ru(bpy)_3^{2+}$doped silica nanoprobe (Au−$RuSiO_2$ NPs) as nanoprobe by Chen et al. The design is feasible and reliable for sensitive insight into the majority of N-glycan expression on the cell surface. (Chen et al. 2013). Gold nanoparticles (AuNPs) was also applied as direct signal transducer probes of luminol for kinase activity analysis. (Xu et al. 2010). The excellent features make nanomaterials are promising in fabrication of ECL biosensor with superior performances.

Tannic acid (TA) is a green and safe nature material contains a number of gallolyl groups, and was used as the basic units for hybrid biomaterial assembly. For example, they can be applied to cross-link the transition metal ions (e.g., Fe^{3+}, Al^{3+}, Cu^{2+}) and

Accepted manuscript

ACCEPTED MANUSCRIPT

series of substrates (e.g., DNA, protein, noble metal nanoparticles, metal oxide particles, cell), (Ejima et al. 2016; Arifur Rahim et al. 2016; Payra et al. 2016; Zhang et al. 2017; Zhang et al. 2017; Alford et al. 2018), the formed cross-linking complex materials can be used in drug delivery, catalysis and coating. (Liang et al. 2016; Zeng et al. 2014; Ejima et al. 2013). Moreover, TA also showed some benefits including antioxidant, antiviral activity, antibacterial, antimutagenic, and reactive oxygen species (ROS) scavengers, et al. (Zhang et al. 2017; Alford et al. 2018), which make it dazzling in biosensing applications.

In this work, a novel ECL biosensor for ultrasensitive detection of HATs activity and inhibitor screening was fabricated by utilizing TA-ferric ions (TA-Fe) complex assembled AuNPs (AuNPs@TA-Fe) as nanoprobes. In this strategy, the substrate peptide modified on electrode can be acetylated in the presence of HATs, and the acetylated peptide was resistance to the hydrolysis of trypsin (Wegener et al. 2003; Marcotte et al. 2004), and can absorb the AuNPs@TA-Fe probe by the hydrophobic interaction and hydrogen bonding interaction. In the presence of luminol, a highly effective ECL indicator with low oxidation potential and inexpensive reagent consumption, the ECL response of the modified electrode in luminol decrease significantly owing the unique features of mimetic SOD of AuNPs@TA-Fe nanoprobe, and can be applied for HATs activity evaluation. The simply fabricated biosensor showed rapid response, high sensitivity and selectivity for HATs acetylation. What's more, the HAT activities assay in complex cell lysates samples were also performed, which showed great potential in clinic diagnostic and HAT-related life science research.

Accepted manuscript

2. Material and methods

2.1 Materials and reagents

Recombinant GST-purified p300 HAT domain, acetyl-coenzyme A (Ac-CoA) and anacradic acid were purchased from Sigma-Aldrich (Shanghai, China). All dilutions solutions of anacardic acid were prepared using anhydrous DMSO as solvent and

further stored at -20 ℃ before use. All peptides were purchased from GL Biochem Ltd. (Shanghai, China). Bovine serum albumin (BSA), hemoglobin and trypsin were obtained from Dingguo Biological Products Co. (Beijing, China). Protein kinase A (PKA) was purchased from New England Biolabs. Tannic acid (TA) were obtained from Alfa Aesar (Shanghai, China). The improved Bradford protein assay dye reagent kit was obtained from Sangon (Shanghai, China). Human breast cancer cells (MCF-7) were provided by the Medicine School of Tsinghua University, Beijing, China. Phosphate buffer solutions (PBS) were prepared with $Na_2HPO_4 \cdot 12H_2O$ and $NaH_2PO_4 \cdot 2H_2O$. All other chemicals of analytical reagent grade were obtained from Beijing Chemical Co. (Beijing, China) and used as received without further purification.

2.2 Apparatus and characterization

The ECL measurements were carried out on an MPI-B multifunctional electrochemical analytical system (Xi'an Remex Analytical Instrument Ltd. Co., China). The voltage of the photomultiplier tube (PMT) was maintained at 500 V. The ECL signal measurement was conducted in PBS solution containing 1 mM H_2O_2 and 100 μM luminol. The cyclic voltammetry (CV) was conducted on a CHI802b instrument (CH Instrument Co., USA). Electrochemical impedance spectroscopy (EIS) was performed on SP-150 (Bio-Logic, France) with the frequency range from 0.1 Hz to 10^5 Hz. Both CV and EIS measured in a solution containing 5 mM of $K_3[Fe(CN)_6]/K_4[Fe(CN)_6]$ probes and 0.1 M KCl. Fluorescence spectra were obtained by using EnVision Multilabel Plate Readers (PerkinElmer, USA). Fourier transform infrared (FT-IR) spectra were obtained on a PerkinElmer Spectrum GX spectrometer (PerkinElmer Co., Waltham, MA).

2.3 The preparation of AuNPs@TA-Fe probe

The AuNPs were prepared by mixing 1 mM chlorchloric acid ($HAuCl_4 \cdot 4H_2O$, 1 mL) and 40 mg mL^{-1} tannic acid (TA, 5 μL), and the mixture was oscillated using vortex mixer at room temperature until the color of mixture turned to red and remained stable

Accepted manuscript

ACCEPTED MANUSCRIPT

over a period time. The prepared AuNPs were centrifugated by centrifuge with a speed of 10000 r/min and collected as stock solution. Secondly, AuNPs@TA-Fe probe was obtained by adding 1 mg mL^{-1} $FeCl_3 \cdot 6H_2O$ (10 μL) into AuNPs stock solution and oscillated at room temperature for 1 min, followed by adding 4 mg mL^{-1} TA (5 μL) with the same condition as the last step. Finally, Tris-HCl (0.5 mL, pH=8.5) was added into the above mixture and the final AuNPs@TA-Fe probe was obtained by centrifuge with a speed of 10000 r/min and washed for three times. The AuNPs@TA-Fe probes with different thickness of shell were prepared by repeated the above steps.

2.4 Biosensor fabrication

A gold electrode was polished successfully by 0.3 μm α-Al_2O_3 power and washed ultrasonically with ethanol and water. After drying with N_2, the bare Au electrode were activated in 0.5 M H_2SO_4 with voltage range from -0.20 to 1.65 V. The activated bare gold electrode was immersed into target peptide (CRGKGGKGLGKGGAKA, 2 μM) solution at 37 °C for 2 h to obtain peptide/Au by the strong interaction between bare Au electrode and cysteine (C), which contain sulfhydryl group (SH) to form Au-S bond. Whereafter, to seal up the nonspecific binding sites, the washed and dried electrode was immersed into mercapto hexanol (MCH, 1 mM) for 1 h to form Au-S bond, and then preformed the HAT p300-catalyzed acetylation reaction by placing the modified electrode in an assay PBS buffer solution containing HAT p300 (100 nM) and acetyl-Co A (Ac-Co A, 30 μM) at 30.5 °C for 2.5 h. After washing with PBS buffer, the electrode was incubated by trypsin solution and obtained the sheared acetylated peptide on the Au electrode surface. Then the modified electrode was immersed into AuNPs@TA-Fe probe solution and the probe absorbed to the electrode surface by the hydrophobic interaction and hydrogen bonding interaction between the sheared acetylated peptide and gallolyl group of TA.

2.5 MCF-7 Cell Culture and Lysate Preparation

Accepted manuscript

ACCEPTED MANUSCRIPT

The MCF-7 cell line was obtained from the Medicine School of Tsinghua University, Beijing, China and was cultured in DMEM medium (Dingguo Biological Products Co., Beijing, China) with 10 % fetal calf serum, 100 U mL^{-1} penicillin, and 100 μg mL^{-1} streptomycin in a humidified atmosphere with 5 % CO_2 at 37 °C. Followed by being replaced in a serum-free medium for 4 h, the cultured cells were scraped and lysed in Dulbecco's phosphate-buffered saline (D-PBS) under sonication (200 W) for 5 min. After being centrifuged for 1 h at 4 °C with a speed of 22000 rpm, the resulting lysate was transferred to freezing tubes as stock solution at −20 °C. With the improved Bradford protein assay dye reagent kit containing BSA as standard, the concentration of total protein in MCF-7 lysate was calculated to be 36 μg mL^{-1}.

3. Results and discussion

3.1 Characterization of the as-prepared AuNPs@TA-Fe probe

The AuNPs@TA-Fe probe with different shell thickness were characterized by UV-vis spectra, as shown in Fig. S1A. From UV-vis spectra, we can see the decrease of absorbance and the red-shift of absorption peak to about 550 nm as the increasing of shell thickness. The fact can be ascribed to the increase of dielectric constant and also indicate the successful preparation of the AuNPs@TA-Fe probe with different shell thickness. What's more, the color of probe solution was also deepening gradually with the increasing shell thickness, which can be seen in Fig. S1B. The phenomemon caused by different fusion of AuNPs, which can be explained by the different degree of interaction between TA assembled nanoprobes with different shell thickness. (Zeng et al. 2014) At the same time, we also characterized the dynamic light scattering (DLS), FT-IR and zetapotential results shown in Fig. S1C, Fig. S1D and Fig. S1E, respectively. From the zeta-potential result, the negative charge of the as-prepared probe may be caused by the AuNPs and phenolic hydroxyl group of TA. Obviously, from FT-IR, we can see the strong peak of phenolic hydroxyl group (about 3200 nm). The facts demonstrated that AuNPs@TA-Fe probes were prepared successfully and its properties could be tuned by the assembly of TA-ferric ion (TA-Fe) complex. Moreover, AuNPs@TA-Fe probes was characterized by XRD, as

Accepted manuscript

ACCEPTED MANUSCRIPT

shown in Fig. S2A. The characteristic peaks of gold nanoparticles can be observed. In addition, the morphology of AuNPs@TA-Fe probe with two layer assembly processes was shown in Fig. S2A. It was observed from the HRTEM picture that the gold nanoparticles with size of ca.35 nm were coated with the TA-ferric ion (TA-Fe) complex of ca. 6nm. The EDX spectra are also shown in Fig. 2C, and the characteristic peaks of Fe, Au can be observed. The TA-Fe complex coated gold nanoparticles were also confirmed by XPS as shown in Fig. S2D. Well defined characteristic peaks of both Au and Fe were also presented, demonstrating the successfully preparation of AuNPs@TA-Fe probes.

3.2 Histone acetyltransferases (HATs) activity evaluation

The principle of the simple turn-off ECL biosensor for the detection of HAT activity was described in Scheme 1.The bare gold electrode was first modified with target peptide by Au-S bond, and followed by blocking with MCH. For comparison, the measurement was divided into experiment group (right) and control group (left). After the acetylation by HATs, the target peptide was resistance to the hydrolysis of trypsin and can absorb AuNPs@TA-Fe probe by the hydrophobic interaction and hydrogen bonding interaction to produce decreased ECL signal of luminol. The as-prepared biosensor was immersed and detected in the solution of luminol and H_2O_2 , and the ECL signals were record in the voltage range from 0 V to 0.6 V with 500 V PMT . In the process of detection, superoxide radical from H_2O_2 was removed by TA assembled probe to induce decreased ECL signal of luminol. The ECL intensities of luminol were closely related with the HATs activity, which was feasible to HATs activity assay and inhibitor screening.

3.3 Characterization of the fabrication of modified Au electrode

Using $[Fe(CN)_6]^{4-/3-}$ as electroactive probes, cyclic voltammetry (CV) and electrochemical impedance spectroscopy (EIS) were used to characterize the assembly procedures on the Au electrode surface. As shown in Fig. 1A, the bare Au

Accepted manuscript

ACCEPTED MANUSCRIPT

electrode exhibited a couple of reversible redox peaks (curve a). After modifying the target peptide, the peak currents were increased (curve b) which could be ascribed to the electrostatic attraction between positive charged target peptide and negative charged electroactive probes. A decreased peak current was observed after the acetylation reaction in the presence of histone acetyltransferases (curve c) and the hydrolysis reaction of trypsin (curve d). The phenomenon may be caused by the charge of target peptide changed from positive to neutral after being acetylated. Finally, the AuNPs@TA-Fe/sheared acetylated peptide/MCH/Au (curve e) showed further decreased current, which may be made by the inner of tannic acid. The above phenomena was also confirmed by the EIS as shown in Fig. 1B. The Nyquist plots were composed of a straight linear at lower frequencies and a semicircular part at higher frequencies, in which the diameter of the semicircular is equal to the electron transfer resistance (Ret). (Qi et al. 2014; Chen et al. 2014) After incubating into target peptide (curve b), the diameter is almost equal to bare Au electrode (curve a), which may be explained by the positive charge of target peptide. It was clear that the diameter of semicircles increased step by step with the assembly of acetylated peptide (curve c), sheared acetylated peptide (curve d) and AuNPs@TA-Fe (curve e), indicating the enhancement of the Ret. These results were consistent with those of CV and demonstrated the feasibility of the simple turn-off biosensor.

3.4 ECL behaviors of the turn-off biosensor

In this strategy, the ECL responses from luminol were closely related with the HAT p300 activity and the mimetic superoxide dismutase (SOD) performance of tannic acid. Fig. 2 shows the ECL response of the target peptide assembled electrode with the treatment of HAT p300 digestion (a) and without the treatment of HAT p300 digestion (b). After the treatment of HAT p300 digestion, the acetylated peptide can absorb more probe and cause lower ECL intensity than the one which without the HAT p300 digestion. In order to further identify the mimetic SOD performance of TA, some control experiments containing the ECL intensity of the electrode without probe

Accepted manuscript

ACCEPTED MANUSCRIPT

treatment (b), with probe treatment (c) after HAT p300 digestion in 100 μM luminol with O_2 and with probe treatment (d) after HAT p300 digestion in 100 μM luminol without O_2 were showed in Fig. 3. It was observed that the ECL signal intensity of the AuNPs@TA-Fe/acetylated peptide/Au was about 4 fold lower that acetylated peptide/Au in luminol, and the ECL intensity of AuNPs@TA-Fe/acetylated peptide/Au in luminol without O_2 was closed to nothing. The above facts demonstrated that the as designed turn-off ECL biosensor can be applied for highly sensitive ECL biosensor for HATs activity detection.

3.5 Optimization of the detection conditions

The effect of digestion time of HAT p300 and the different thickness shell of AuNPs@TA-Fe probe on the ECL response of the modified electrode was important and also studied. As shown in Fig. S3 in the supporting information, the ECL current decreased with the increasing of HATs digestion time, and reached a plateau at 150 min. In order to optimize the shell thickness of the as-prepared probe, the ECL intensity of different shell thickness of the as-prepared probe was showed in Fig. S4. As the increasing of shell thickness, the ECL intensity reached a plateau with two cycles thickness of as-prepared probe shell. Thus, 150 min for histone proteins acetylation and two cycles thickness of as-prepared probe shell were chosen in the HATs activity study.

3.6 ECL measurements of HATs activity and selectivity of the turn-off biosensor

The assessment of HATs activities was carried out under the above optimized experimental conditions. For HAT p300 activity detection, the peptide/Au was incubated by a series PBS buffer containing HAT p300 with different concentration (0, 0.1, 1, 5, 7.5, 10, 25, 50, 75, 100, 500 and 1000 nM) and Ac-Co A (30 μM). After acetylation reaction, the electrode was modified and used for ECL measurement with the same conditions above mentioned. Each experiment under different concentration of HATs was performed at least three times. From 0 to 0.6 V, the ECL-potential curves

Accepted manuscript

ACCEPTED MANUSCRIPT

and the stability of the biosensor towards different HAT p300 concentrations (25, 50 and 75 nM as example) were shown in Fig. S5. In detail, the ECL responses of luminol toward different concentrations of HAT p300 were shown in Fig. 4. The ECL intensity decreased as the increasing concentrations of HATs, and reached a plateau. A good linear relationship was obtained at the concentrations range from 0.1 to 100 nM with a regression coefficient (R) of 0.983, and the detection limit was 0.074 nM (S/N=3). (Hu et al. 2015; Chen et al. 2015). A comparative table of the previous reported work and this work was shown in Table S1.

By adding protein kinase A (PKA), bull serum albumin (BSA), hemoglobin and mixture (including PKA, hemoglobin and HAT p300) instead of HAT p300, the selectivity of the turn-off ECL biosensor was also investigated (Fig. S6). Under the same experimental conditions, the ECL intensities of the alternative proteins added were nearly the same as that of blank samples without addition of the HAT p300 even though their concentrations were 10 times higher than that of HAT p300. The ECL intensity of samples by adding mixture was nearly the same as that of samples with addition of HAT p300, indicating the adding of PKA, BSA and hemoglobin was no effect in the acetylation reaction of HAT p300. The fact indicated that the as-designed turn-off ECL biosensor presented excellent selectivity toward HAT p300 activity evaluation.

3.7 Inhibition evaluation and HATs activity detection in cell lysates

Considering the vital role of HATs in many diseases, such as cancer, HIV infection and inflammatory, a sensitive and highly analysis approach for screening of HAT inhibitors is crucial. Anacardic acid, a potent small molecule inhibitor of HAT p300, was selected as an example to test the feasibility of the as-designed turn-off biosensor for drug screening. (Han et al. 2015; Hu et al. 2015) For HAT p300 inhibition analysis, firstly, the peptide/Au was incubated with mixture including HAT p300 (100 nM) and inhibitor anacardic acid with different concentrations for 10 min at room temperature. And the final concentrations of anacardic acid were 1.0, 5.0, 10, 25, 50, 75, 100, 500, and 1000 μM, respectively. Followed by the adding of Ac-Co A (30 μM), the

Accepted manuscript

ACCEPTED MANUSCRIPT

screening of HAT p300 inhibitor was initiated at 30 °C for 2.5 h. Finally, the following experiment processes were taken out as described above. It was observed that the ECL signals of the as-designed turn-off biosensor increased by increasing the concentration of anacardic acid. The ECL responses as a function of the logarithms of the HAT p300 concentrations were plotted as shown in Fig. 5, from which the IC_{50} value of inhibitor anacardic acid toward HATs was calculated to be 59.06 μM, which was comparable to those reported previously. (Xie et al. 2009; Hu et al. 2015; Chen et al. 2015) The facts manifested that the turn-off ECL biosensor was feasible to qualitatively inhibitor screening of the HATs.

In lysate samples of MCF-7 cancer cell, the activity assessment of HAT p300 with different concentrations was also conducted under the same conditions. As shown in Fig. S7A, the linear range was from 1 to 100 nM and the regression coefficient (R) was 0.996. Using the improved Bradford protein assay dye reagent kit containing BSA as standard, the concentration of total protein in MCF-7 cell lysate was calculated to be 36 μg mL^{-1} (Fig. S7B). The recovery ranged from101% to 102% was obtained and displayed in Table S2. The above facts clearly indicated that the turn-off ECL biosensor is potential and feasible to be used in real biological samples.

Accepted manuscript

Conclusions

In summary, a novel ECL biosensing platform was developed for the detection of HATs activity and inhibitor screening. By combining the anti-hydrolysis ability of acetylated peptide and mimetic superoxide dismutase of tannic acid assemble nanoprobes, the as designed ECL biosensor exhibited highly sensitive to the HATs activity analysis with a detection limit of 0.074 nM. In addition, it can also be applied in the biological samples analysis with excellent selectivity. The inhibitor screening of HATs were also performed with high accuracy, which can contribute to the discovery of anti-cancer drug, the understanding of chemotherapy and biochemical research.

ACCEPTED MANUSCRIPT

Acknowledgments

This work was financially supported by National Key Research and Development Program of China (No.2016YFA0203101), National Natural Science Foundation of China (No. 21622506, 21375073, 21235004, 21621003, 21475071), Tsinghua University Initiative Scientific Research Program (2014z21027), Beijing municipal science and technology commission (Z171100001117135) and the Taishan Scholar Program of Shandong Province (ts201511027).

References

Li, P., Han, Y.T., Li, Y., Zhu, R., Wang, H.X., Nie, Z., Yao, S.Z., 2016. Anal. Bioanal. Chem. 408(11), 2659-2668.

Zhen, Z., Tang, L.J., Long, H.X., Jiang, J.H., 2012. Anal. Chem. 84(8), 3614-3620.

Kim, Y., Tanner, K.G., Denu, J.M., 2000. Anal. Biochem. 280(2), 308-314.

Dancy, B.M., Cole, P.A., 2015. Chem. Rev. 115(6), 2419-2452.

Ghadiali, J.E., Lowe, S.B., Stevens, M.M., 2011. Angew. Chem. 123(15), 3479-3482.

Han, Y.T., Li, H., Hu, Y.F., Li, P., Wang, H.X., Nie, Z., Yao, S.Z., 2015. Anal. Chem. 87(18), 9179-9185.

Han, Y.T., Li, P., Xu, Y.T., Li, H., Song, Z.L., Nie, Z., Chen, Z., Yao, S.Z., 2015. Small 11(7), 877-885.

Xie, N., Elangwe, E.N., Asher, S., Zheng, Y.G., 2009. Bioconjugate Chem. 20(2), 360–366.

Hu, Y.F., Chen, S.Y., Han, Y.T., Chen, H.J., Wang, Q., Nie, Z., Huang, Y., Yao, S.Z., 2015. Chem. Commun. 51, 17611-17614.

Chen, S.Y., Li, Y., Hu, Y.F., Han, Y.T., Huang, Y., Nie, Z., Yao, S.Z., 2015. Chem. Commun. 51, 4469-4472.

Li, J., Hong, X., Li, D., Zhao, K., Wang, L., Wang, H.Z., Du, Z.L., Li, J.H., Bai, Y.B., Li, T.J., 2004. Chem. Commun. 0, 1740-1741.

Zhang, L., Zhang, Q., Lu, X.B., Li, J.H., 2007. Biosens. Bioelectron. 23(1), 102-106.

Accepted manuscript

ACCEPTED MANUSCRIPT

Zhang, Y.J., Wen, Y., Liu, Y., Li, D., Li, J.H., 2004. Electrochem. Commun. 6(11), 1180-1184.

Yang, L.L., Tao, Y.Z., Yue, G.Y., Li, R.B., Qiu, B., Guo, L.H., Lin, Z.Y., Yang, H.H., 2016. Anal. Chem. 88(10), 5097-5103.

Qi, H.L., Li, M., Dong, M.M., Ruan, S.P., Gao, Q., Zhang, C.X., 2014. Anal. Chem. 86(3), 1372-1379.

Divsar, F., Ju, H.X., 2011. Chem. Commun. 47(35), 9879-9881.

Shi, C.G., Shan, Y., Xu, J.J., Chen, H.Y., 2010. Electrochim. Acta 55(27), 8268-8272.

Chen, Z.H., Liu, Y., Wang, Y.Z., Zhao, X., Li, J.H., 2013. Anal. Chem. 85(9), 4431-4438.

Li, J., Cheng, G., Dong, S., 1996. J. Electroanal. Chem. 416(1-2), 97-104.

Lu, X., Wen, Z., Li, J., 2006. Biomaterials 27(33), 5740-5747.

Hu, J., Wang, Z., Li, J., 2007. Sensors 7(12), 3299-3311.

Wang, Y., Li, Z., Weber, T., Hu, D., Lin, C., Li, J., Lin, Y., 2013. Anal. Chem. 85, 6775-6782.

Wang, Y., Tang, L., Li, Z., Lin, Y., Li, J., 2014. Nat. Protoc. 9(8), 1944-1955.

Zhang, Q., Qiao, Y., Hao, F., Zhang, L., Wu, S., Li, Y., Li, J., Song, X., 2010. Chem. Eur. J. 16(27), 8133-8139.

Forzani, E.S., Lu, D., Leright, M.J., Aguilar, A., Tsow, F., Iglesias, R.A., Zhang, Q., Lu, J., Li, J., Tao, N., 2009. J. Am. Chem. Soc., 131(4), 1390–1391.

He, Y., Li, J.H., Liu, Y. 2015. Anal. Chem. 87(19), 9777-9785.

Wang, Y.Z., Chen, Z.H., Liu, Y., Li, J.H., 2013. Nanoscale 5(16), 7349-7355.

Yang, G.H., Zhu, C.Z., Du, D., Zhu, J.J., Lin, Y.H., 2015. Nanoscale 7(34), 14217-14231.

Liu, Y., Liu, Y., Feng, H.B., Wu, Y.M., Joshi, L., Zeng, X.Q., Li, J.H., 2012. Biosens. Bioelectron. 35(1), 63-68.

Chen, X.J., He, Y., Zhang, Y.Y., Liu, M.L., Liu, Y., Li, J.H., 2014. Nanoscale 6(19), 11196–11203.

Xu, S.J., Liu, Y., Wang, T.H., Li, J.H., 2010. Anal. Chem. 82(22), 9566-9572.

Ejima, H., Richardson, J. J., Caruso, F., 2016. Nano Today 12. 136-148.

Accepted manuscript

ACCEPTED MANUSCRIPT

Arifur Rahim, M., Björnmalm, M., Suma, T., Faria, M., Ju, Y., Kempe, K., Müllner, M., Ejima, H., Stickland, A. D., Caruso, F., 2016. Angew. Chem. Int.Ed. 55(44), 13803-13807.

Payra, D., Naito, M., Fujii, Y., Nagao, Y., 2016. Chem. Commun. 52(2), 312-315.

Zhang, J.P., Cui, L.J., Han, X., Zhang, Y.Y., Zhang, X., Chu, X., Zhang, F.H., Zhang, Y., Chu, L., 2017. Biomed. Pharmacother. 93, 1253-1260.

Zhang, J.P., Song, Q.T., Han, X., Zhang, Y.Y., Zhang, Y., Zhang, X., Chu, X., Zhang, F.H., Zhang, Y., Chu, L., 2017. Int.Immunopharmacol. 47, 95-105.

Alford, A., Kozlovskaya, V., Xue, B., Gupta, N., Higgins, W., Pham-Hua, D., He, L., Urban, V.S., Tse, H.M., Kharlampieva, E., 2018. Chem. Mater. 30(2), 344-357.

Wegener, D., Wirsching, F., Riester, D., Schwienhorst, A., 2003.Chem. Biol. 10, 61–68.

Marcotte, P.A., Richardson, P.R., Guo, J., Barrett, B.W., Xu, N., Gunasekera, A., Glaser, K.B., 2004. Anal. Biochem. 332, 90–99.

Liang, H., Li, J., He, Y., Xu, W., Liu, S., Li, Y., Chen, Y., Li, B., 2016. ACS Biomater. Sci. Eng. 2(3), 317–325.

Zeng, T., Zhang,X. Guo, Y., Niu, H., Cai, Y., 2014. J. Mater. Chem. A 2(36), 14807–14811.

Ejima, H., Richardson, J.J., Liang, K., Best, J.P., van Koeverden, M.P., Such, G.K., Cui, J., Caruso, F., 2013. Science 341(6142), 154–157.

Liu, T., Zhang, L.C., Song, H.J., Wang, Z.H., Lv, Y., 2013. Luminescence 28(4), 530-535.

Chen, A., Ma, S.Y., Zhuo, Y., Chai, Y.Q., Yuan, R., 2016. Anal. Chem. 88(6), 3203-3210.

Sharon, E., Enkin, N., Albada, H.B., Willner, I., 2015. Chem. Commun. 51(6), 1100-1103.

Huang, J., Wang, H., Yang, X.H., Yang, Y.J., Quan, K., Ying, L., Xie, N.L., Ou, M., Wang, K.M., 2016. Chem. Commun. 52(2), 370-373.

Miao, P., Tang, Y.G., Yin, J., 2015. Chem. Commun. 51(86), 15629-15632.

Accepted manuscript

ACCEPTED MANUSCRIPT

Ge, Z.L., Lin, M.H., Wang, P., Pei, H., Yan, J., Shi, J.Y., Huang, Q., He, D.N., Fan, C.H., Zuo, X.L., 2014. Anal. Chem. 86(4), 2124-2130.

Chen, X.J., Wang, Y.Z., Zhang, Y.H., Chen, Z.H., Liu, Y., Li, Z.L., Li, J.H., 2014. Anal. Chem. 86(9), 4278-4286.

Fig 1. Cyclic voltammograms (A) and electrochemical impedance spectra (B) of (a) bare Au, (b) peptide/Au, (c) acetylated peptide/MCH/Au, (d) sheared acetylated peptide/MCH/Au, (e) AuNPs@TA-Fe/ sheared acetylated peptide/MCH/Au.

Fig 2. Contrasted ECL intensity-time curves of the turn-off biosensor in response to amino acid/MCH/Au (b) and AuNPs@TA-Fe/acetylated peptide/MCH/Au (a).

Fig 3. ECL intensity-time curves of bare Au (a), acetylated peptide/Au (b), AuNPs@TA-Fe/acetylated peptide/Au in 100 μM luminol (c) and AuNPs@TA-Fe/acetylated peptide/Au in 100 μM luminol without O_2 (d).

Fig 4. ECL intensity-time curves of the turn-off biosensor in response to increasing concentrations of HAT p300. (From top to bottom: 0, 0.1, 1, 5, 7.5, 10, 25, 50, 75, 100, 500 and 1000 nM). And the inset is optimization experiments and its calibration curve of the biosensor to various concentrations of HAT p300.

Fig 5. Detection of HAT inhibition by the turn-off biosensor. From left to right: anacardic acid, 1.0, 5.0, 10, 25, 50, 75, 100, 500, and 1000 μM .The ECL signal curve as a function of the concentration of anacradic acid.

Scheme 1. The principle of the proposed ECL biosensor for HATs activity detection.

Accepted manuscript

ACCEPTED MANUSCRIPT

Figure 1.

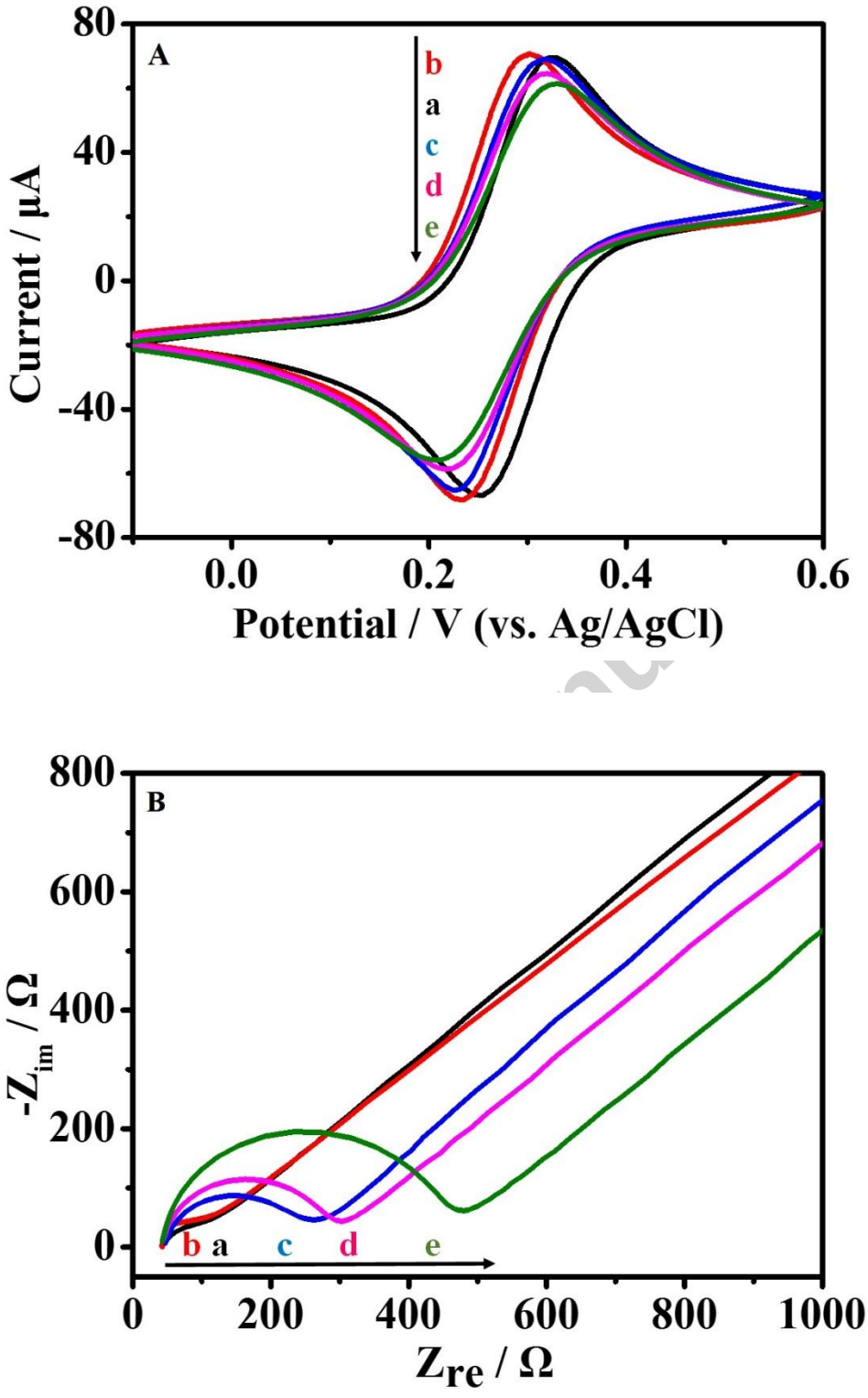

ACCEPTED MANUSCRIPT

Figure 2.

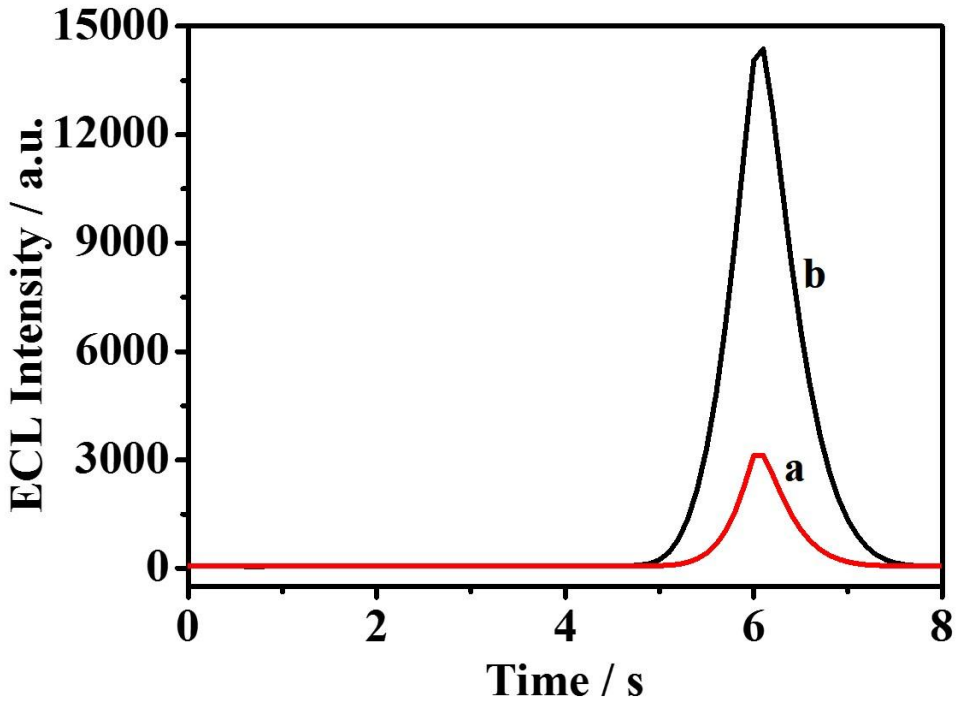

Accepted manuscript

ACCEPTED MANUSCRIPT

Figure 3.

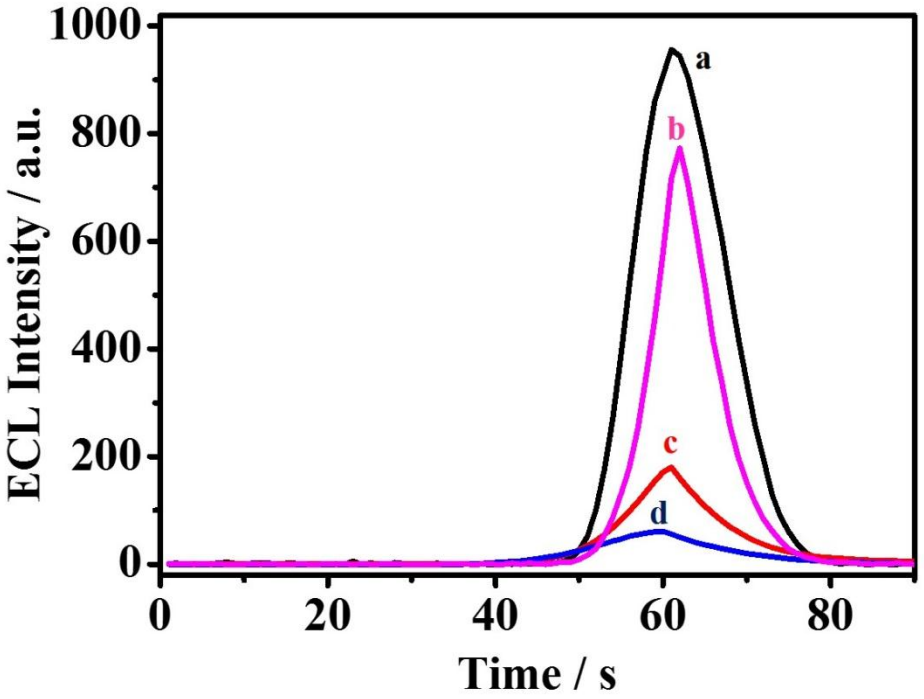

Accepted manu

ACCEPTED MANUSCRIPT

Figure 4.

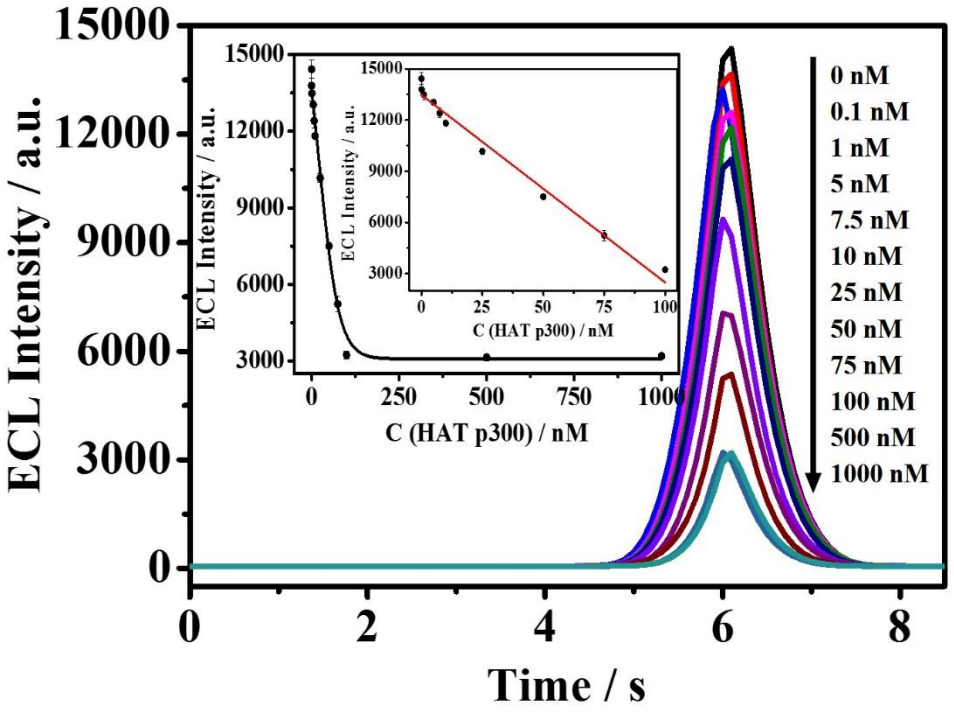

Accepted manuscript

Figure 5.

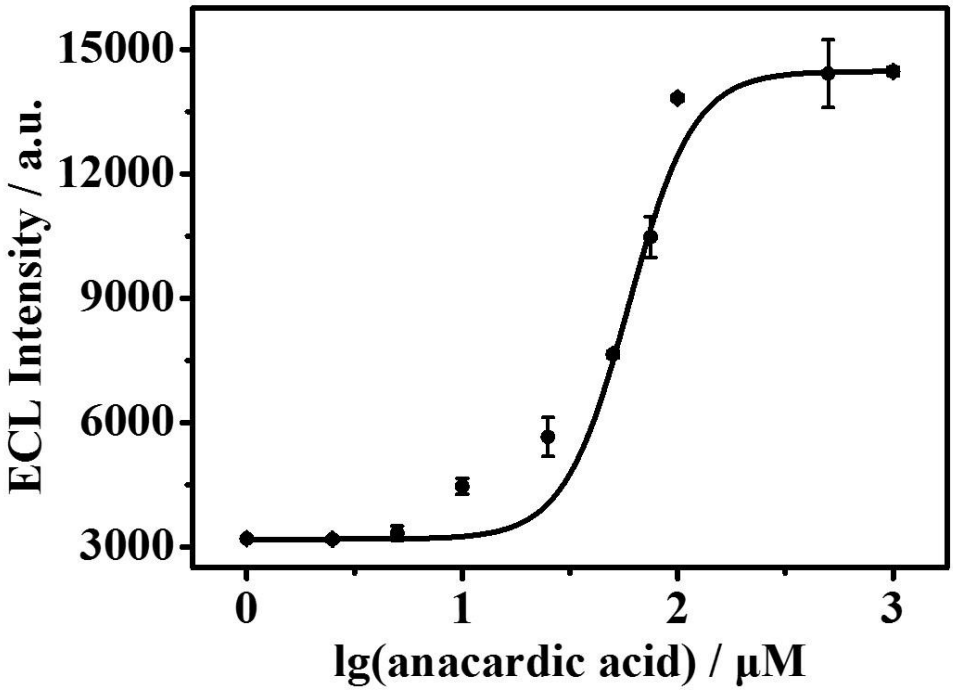

Scheme 1.

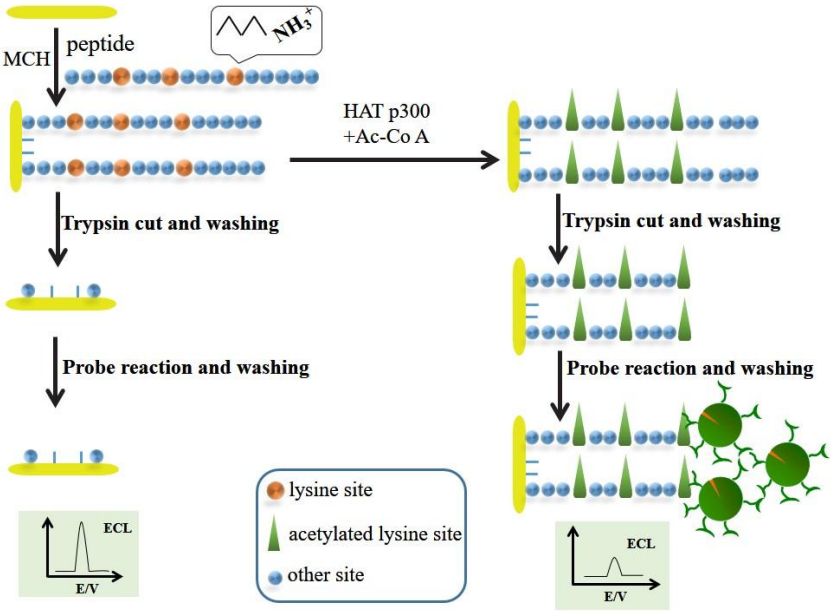

ACCEPTED MANUSCRIPT

Highlights

- A turn-off ECL biosensor for HATs activity analysis and inhibition was first designed.
- Mimetic SOD features of TA assembled AuNPs nanoprobes was successfully prepared.
- A strategy based on mimetic SOD nanoprobes was developed with sensitivity and selectivity.
- The biosensor was applied in cell lysates and showed promise in HATs-related research.

Accepted manuscript